Applied Physics A (2018) 124:486
https://doi.org/10.1007/s00339-018-1904-y

Applied Physics A
Materials Science & Processing

Polarizability, optical basicity and optical properties of $SiO_2B_2O_3Bi_2O_3TeO_2$ glass system

I. Kashif[2] · A. Ratep[1] · Gh. Adel[2]

Received: 4 February 2018 / Accepted: 7 June 2018 / Published online: 11 June 2018

Abstract
Glasses having a composition $x SiO_2 x B_2O_3$ $(95-2x)$ $Bi_2O_3 5TeO_2$ where $x = (5, 10, 15, 20, 25)$ prepared by the melt-quenching technique. Thermal stability, density, optical transmittance, and the refractive index of these glasses investigated. Glass samples were transparent in the visible to near-infrared (NIR) region and had a high refractive index. A number of glass samples have high glass-forming ability. This indicates that the quarterly glasses are suitable for optical applications in the visible to the NIR region. Bi_2O_3 substituted by B_2O_3 and SiO_2 on optical properties discussed. It suggested that the substitution of Bi_2O_3 increased the density, molar volume, the molar polarizability, optical basicity and refractive index in addition to, the oxygen packing density, the optical energy gap, and metallization decrease. These results are helpful for designing new optical glasses controlled to have a higher refractive index. All studied glass presented high nonlinearities, and the addition of network modifiers made a little contribution. Results clarified the bandgap energy reduction, which associated with the growth within the non-bridging oxygen content with the addition of the network modifier. An increase in the refractive index nonlinearity explained by the optical basicity and the high electronic polarizability of the modifier ions.

1 Introduction

According to a technological and scientific application of Bismuth borate glasses [1–3], these glasses become interesting materials for structural, optical and electrical investigations [4–7]. Tasheva and Dimitrov [8] studied the nonlinear optical properties of TeO_2 Bi_2O_3 B_2O_3 oxide glasses. It established that the glasses posses' high third-order nonlinear susceptibility in the $(0.64–2.31 \times 10^{-13}$ esu) range. Lin et al. [9] studied the ultra nonlinear properties of Bi_2O_3 B_2O_3 oxide glass, they found that the nonlinear response time is lesser than 90 femtosecond and the nonlinear refractive index estimated to 1.6×10^{-14} cm^2/W.

Adding composition compounds containing lone pairs ions or ions unoccupied *d*-orbital to the glass samples increased the nonlinear optical properties of oxide glass. Metal and semiconductor nano-particles (Si, Cu, Ge, and Bi)-doped glasses prepared by the melt-quenching method display large third-order optical nonlinearity [10, 11]. Third-order nonlinearity of some promising oxide glasses were investigated and developed [12]. Optical properties [13] of silicate, borosilicate, telerate and heavy metal oxide glasses were studied. Several studies found that the nonlinear optical properties are created in the all-glass system. A number of researchers investigated the nonlinear optical properties of borate glass. Borate glasses have photonic properties which contain a transparent, low glass transition temperature (T_g), high density, high thermal expansion coefficient and high vitrifying ability besides the ability to dissolve large quantities of other glass formers, modifiers, intermediate, rare-earths and metal nano-particles without reduction of the glass-forming ability. Optical non-linearity of Bi_2O_3-based glasses are increasing by the addition of either a second lone pair holder (such as Te^{4+}, Pb^{2+}) or cations with empty *d*-orbital (such as W^{6+}, Ti^{4+}, Nb^{5+}) [14]. Silicon tetrahedra SiO_4 has similar behavior observed with transition metals having either a d^0 or d^{10} electronic.

No systematic study has been done for $SiO_2B_2O_3Bi_2O_3TeO_2$ glasses, so far, so in the present article we report the optical properties of $x SiO_2$ $x B_2O_3$ $(95-2x)$ Bi_2O_3 $5TeO_2$ where $x = (5, 10, 15, 20, 25)$.

✉ I. Kashif
ismailkashif52@yahoo.com

[1] Faculty of Girls, Department of Physics, Ain Shams University, Heliopolis, Cairo, Egypt

[2] Faculty of Science, Department of Physics, Al-Azhar University, Nasr City, Cairo, Egypt

2 Experimental

Glasses having a composition $x\mathrm{SiO_2}$ $x\mathrm{B_2O_3}$ $(95-2x)$ $\mathrm{Bi_2O_3}$ $5\mathrm{TeO_2}$ where $x = (5, 10, 15, 20, 25)$ prepared by the conventional melt-quench technique. Raw materials have employed: $\mathrm{SiO_2}$ (Sherwood Medical USA, 99.99%), $\mathrm{Bi_2O_3}$ (STREM Chemical, USA 99.9%), $\mathrm{H_3BO_3}$ (Merck Germany, 99.8%), TeO2 (STREM Chemical, USA 99%). $\mathrm{SiO_2}$, $\mathrm{B_2O_3}$, $\mathrm{Bi_2O_3}$, and $\mathrm{TeO_2}$ weighted (10 g) in molar ratio and mixed in an agate mortar to obtain a homogeneous fine powder.

The mixture was melted in a porcelain crucible using an electric furnace at 1100 °C for half hour. Then, the melt-quenched is pouring on a copper plate and subsequently pressing it with another at room temperature. Differential thermal analysis (DTA) (Shimadzu 50) used to obtain the glass-transition temperature T_g, crystallization temperature T_c, and melting temperature T_m with a heating rate 25 °C $\mathrm{min^{-1}}$ in the temperature range of 20–1000 °C, using $\mathrm{Al_2O_3}$ as a reference.

Optical transmission spectra for all the studied glass samples recorded using a computerized recording spectrophotometer (type JASCO, V-570). Glass sample density determined to use the Archimedes method. Glass sample was weighed in the air and in toluene three times at room temperature (25 °C). The density determined by the equation is:

$$\rho = 0.8635 \left[W_a / \left(W_a - W_b\right)\right]$$

where ρ is the density of the glass sample, W_a is the weight of the glass sample in air, W_b is the weight of the glass sample in toluene and 0.8635 is the density of toluene.

3 Results and discussions

3.1 Density and DTA studies

As-prepared glass samples were transparent and dark yellow color. Figure 1 shows the photographs of glass samples as prepared.

Figure 2 shows the scanning electron microscope (SEM) images of $x\mathrm{SiO_2}x\mathrm{B_2O_3}$ $(95-2x)$ $\mathrm{Bi_2O_3}5\mathrm{TeO_2}$ where $x = (5$ and 25) glass samples and the percentages of the elements present in the studied glass samples obtained using the energy-dispersive X-ray spectra (EDS). The morphologies of these glass samples confirming the amorphous nature of the glass sample.

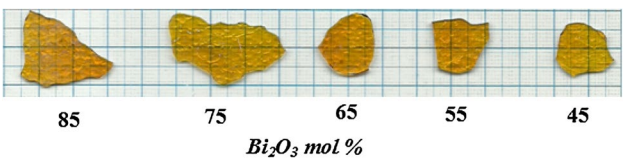

Fig. 1 Photograph of as-prepared glass samples

Figure 3 shows the relation between the (theoretical and experimental) density and bismuth oxide content.

Figure 3 demonstrates that the density increases as the increase of $\mathrm{Bi_2O_3}$ content due to the $\mathrm{Bi_2O_3}$ molecular weight (465.96 g/mol) greater than the $\mathrm{B_2O_3}$ molecular weight (69.6182 g/mol) and $\mathrm{SiO_2}$ molecular weight (60.08). In addition, the molar volume increases as the $\mathrm{Bi_2O_3}$ content increase as appeared in Fig. 4.

This increase attributed to the atomic radii and bond length of $\mathrm{Bi_2O_3}$ larger than those of $\mathrm{B_2O_3}$ and $\mathrm{SiO_2}$ thus caused the expansion of free volume [15]. For instance, Bi^{3+} ions act as the modifier in the network structure in the $\mathrm{Bi_2O_3}$–$\mathrm{B_2O_3}$ glass when $\mathrm{Bi_2O_3}$ content is over 45 mol% [16] and the emerging ($\mathrm{BiO_6}$) structure of a high $\mathrm{Bi_2O_3}$ content play the same role in the glass. Another possible reason for the confusion is the closeness or coincides of the Si–O in the glass network with that of the Bi–O and B–O units [17, 18].

Oxygen packing density (OPD) determines the arrangement of the oxygen atoms in glass network. OPD is calculated using the relation [19–21].

$$\mathrm{OPD} = 1000 \times \mathrm{O/Vm}$$

where 'O' represents the sum of oxygen in the oxide glass component. OPD determines and is represented in Fig. 5. From Fig. 5, it observed that the oxygen packing density decrease with the $\mathrm{Bi_2O_3}$ concentration increase.

But the molar volume has the opposite behavior. The OPD value decrease indicates the conversion of $\mathrm{BO_4}$ to $\mathrm{BO_3}$ that initiate the increase in the bridging oxygen that makes the glass more open structured.

The thermal curves obtained (DTA) for all the studied samples are displayed in Fig. 6.

The thermal spectrum of DTA contains distinct transitions such as glass-transition temperature (T_g) which indicates a transition from a rigid to flexible structure. The second transition is crystallization temperature (T_c) observed as an exothermic peak. The third transition is melting temperature (T_m), which of course is an endothermic peak. Table 1 represents the values of T_g, T_c, and T_m for all the studied samples. It is clear that the transition temperature values [T_g, T_c, T_m] decrease with increasing the $\mathrm{Bi_2O_3}$ content. Which results in the splitting of the glass network former bonds and for this reason the bridging oxygen changed into non-bridging oxygen and the glass structure becomes a weakness [22].

The values of glass-transition temperature decrease caused by the increase of the Bi–O bond which is weaker than that of other glass former bond strength (Si–O and B–O) [22, 23]. Now, it is essential to calculate the average single-bond strength for all the studied glasses. The average single-bond strength B_{M-O} determined as follows: [24, 25],

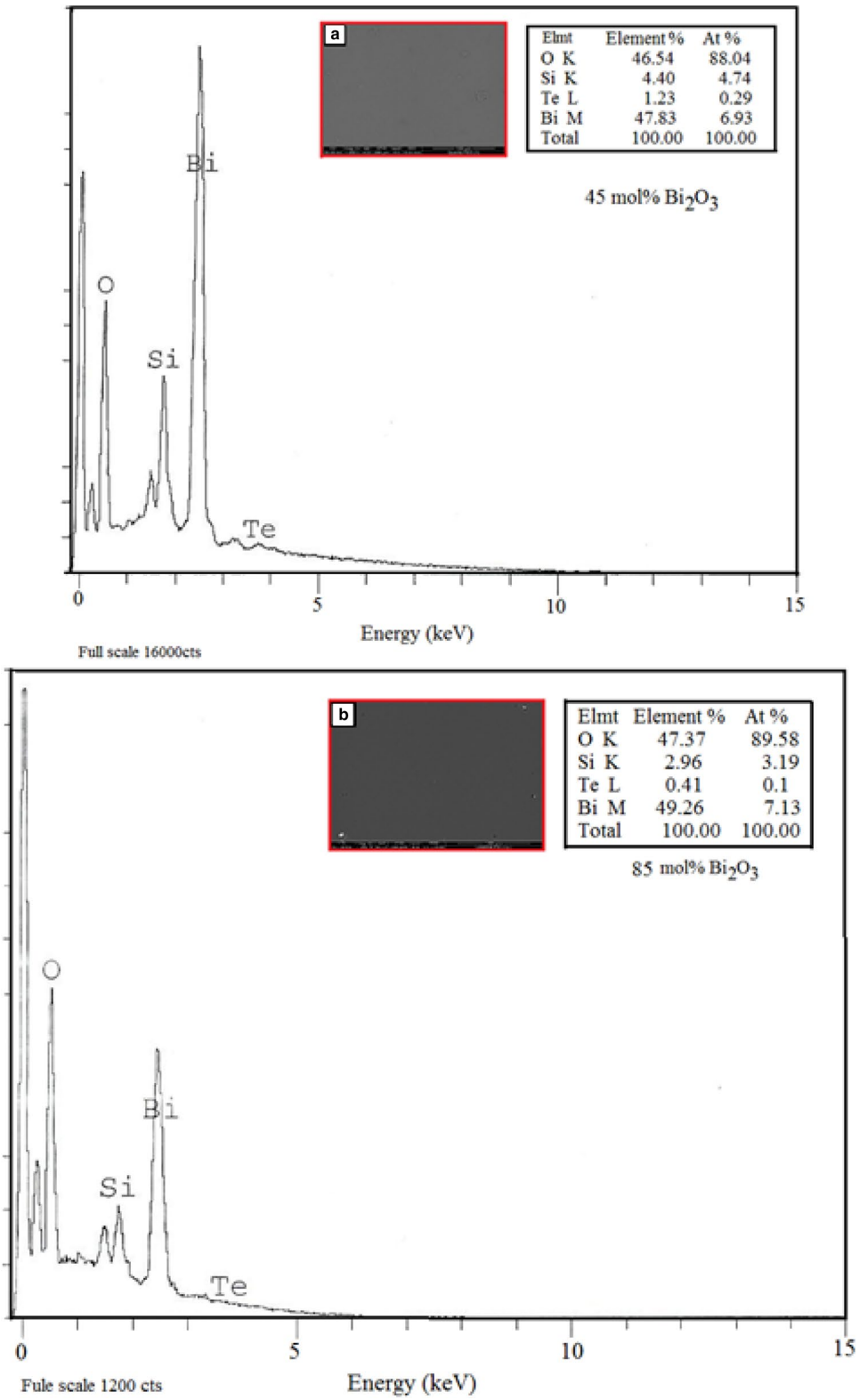

Fig. 2 The scanning electron microscope (SEM) images of $xSiO_2xB_2O_3$ $(95-2x)$ $Bi_2O_35TeO_2$ where $x = (5$ and $25)$ glass samples the percentages of the elements present in the studied glass samples obtained using the energy-dispersive X-ray spectra (EDS)

$$B_{M-O} = x_{SiO_2}B_{Si-O} + x_{B_2}O_3B_{Bi-O} + x_{TeO_2}B_{Te-O}$$

where x_{SiO_2} is the molar fraction of SiO_2, x_{B2O_3} is the molar fraction of B_2O_3, $x_{Bi_{2O_3}}$ is the molar fraction of Bi_2O_3 and x_{TEO_2} is the molar fraction of TeO_2. The single-bond strength of Si–O, B–O, Bi–O and Te–O are 443, 373, 102.5 and 391 KJ/mol, respectively.

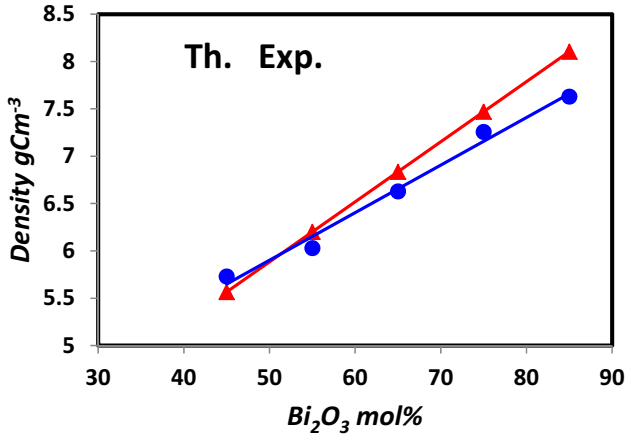

Fig. 3 The relation between the theoretical and experimental density as a function of bismuth oxide content

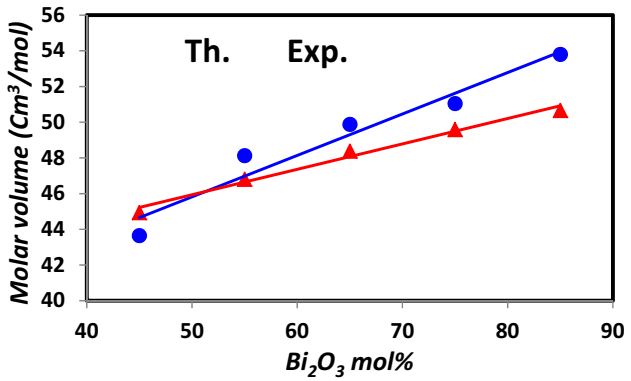

Fig. 4 Variation of the theoretical and experimental molar volume (Vm) with Bi_2O_3 content for xB_2O_3–(95−2x) Bi_2O_3–$xSiO_2$–5TeO_2 glass system

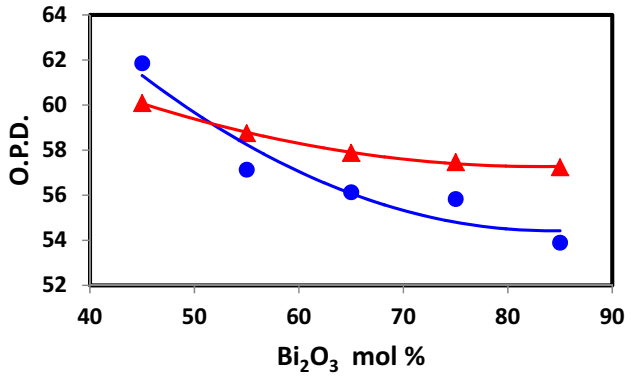

Fig. 5 The relation between the OPD as a function of bismuth oxide content

Table 1 shows the average single-bond strength for the glass samples. It is clear that the values of average single bond decrease by increasing the Bi_2O_3 content.

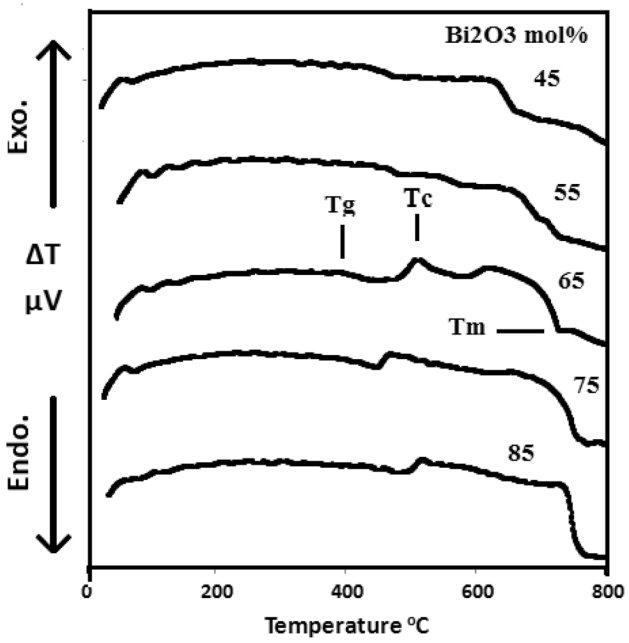

Fig. 6 DTA curves for different xB_2O_3–(95−2x) Bi_2O_3–$xSiO_2$–5TeO_2 glass compositions

Hruby's parameter [26], $K_{gL} = (T_c - T_g)/(T_m - T_c)$, evaluated for studying samples. Hruby's parameter gives information concerning the stability of glass sample against nucleation and crystal growth. At $K_{gL} > 0.1$, it suggests that the glass samples are good glass formers [26]. Table 1 clears that the glass-forming ability, K_{gL}, for the studied samples decrease by increasing Bi_2O_3 content and greater than 0.1.

3.2 Optical properties

Figure 7 shows the optical transmission spectrum for xB_2O_3–$xSiO_2$–(95−2x) Bi_2O_3 5TeO_2 where x = (5, 10, 15, 20 and 25) glass samples. The absorption coefficient α of each sample determined to use the relation [27].

$$\alpha = (\ln I_o/I_t)/d$$

where I_o and I_t are the intensities of the incident and transmitted radiation and d is the sample thickness. Mott and Davis [28] proposed the relation between the absorption coefficient $\alpha(\omega)$ and the photon energy $\hbar\omega$ of the incident radiation, this relation is written as follows:

$$\alpha h\omega = \beta(h\omega - E_{opt})^n$$

where ω is the angular frequency of radiation, β is constant (band parameter), E_{opt} is the optical energy gap (Tauc's method) and n equal 2, 3, 1/2, 3/2 transition process, $n = 1/2$, 2 for a direct, indirect allowed transition, $n = 3/2$, 3 for a direct, indirect forbidden transition. Plots of $\alpha\hbar\omega$, $(\alpha\hbar\omega)^{1/2}$,

Table 1 Transition temperature T_g, T_c, T_m, values of glass-forming ability Kgl and the values of the average single bond strength B–O for all the studied glasses

Sample	T_g (K)	T_c (K)	T_m (K)	K_{gL}	B–O (KJ/mol)
$25SiO_225B_2O_545Bi_2O_35T_eO_2$	703	823	963	0.86	269. 7
$20SiO_220B_2O_555Bi_2O_35T_eO_2$	713	783	993	0.33	239.0
$15SiO_215B_2O_565Bi_2O_35T_eO_2$	663	778	993	0.53	208.6
$10SiO_210B_2O_575Bi_2O_35T_eO_2$	653	738	1043	0.28	178.0
$5SiO_25B_2O_585Bi_2O_35T_eO_2$	693	788	1043	0.37	147. 5

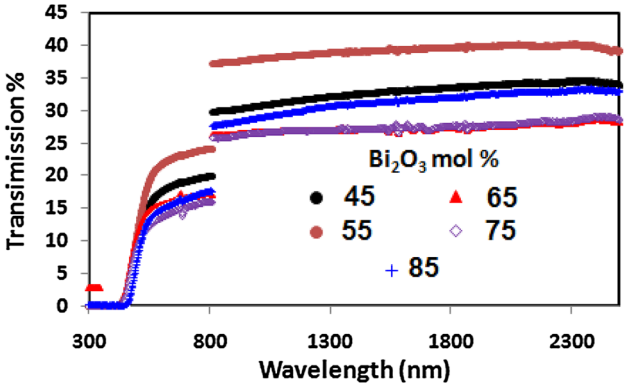

Fig. 7 The optical transmission spectra of the studied glass samples

$(\alpha\hbar\omega)^{3/2}$, $(\alpha\hbar\omega)^2$ $(\alpha\hbar\omega)^{1/3}$, against the photon energy obtained.

The optical energy gap (E_{opt}) value for samples containing 45 and 85 mol% Bi_2O_3 as an example definite from the meeting point between $(\alpha\hbar\omega)^{1/n}$ and $\hbar\omega$ as exposed in Fig. 8. In addition, the optical band gap $E_{opt}(\lambda_g)$ (photon energy's method) determined using the expression from the cutoff wavelength λ_g [29, 30].

$$E_{opt}(\lambda_g) = \frac{1239.38}{\lambda_g}$$

The optical band gap values $E_{opt}(\lambda_g)$ of present glass samples calculated using the values of the cutoff wavelength λ_g. From observing the optical band gap E_{opt} far from the $E_{opt}(\lambda_g)$ It indicates that the E_{opt} method does not correct for all compounds. $E_{opt}(M)$ is determined from the absorption coefficient α or n or k, and found that the optical band gap$E_{opt}(M)$ is closed to $E_{opt}(\lambda_g)$ and is more accurate.

And from the equation, $\ln(ahv) = \ln B + n\ln\{hv - E_{opt}(M)\}$ determined the weather of transition [31].

Table 2 is clear that the decreasing of optical band gap energy value by increasing Bi_2O_3 content. Optical band gap energy decreasing due to the bond strength of bismuth oxide is lower than silicon oxide and boron oxide bond strength besides the increasing number of non-bridging oxygen indicates the increasing number of free electrons [32]. The Urbach energy gives the width of the tails of the localized states within the optical energy gap. The dependence of the absorption coefficient in the region of lower photon energy of the absorption edge is described by the following formula [33]:

$$\alpha h\omega = \beta\ \exp(h\omega/\cup)$$

where ∪ is the Urbach energy. The value of the Urbach energy ∪ is calculated from the reciprocal of the slope of the linear portion of drawn the relation between ln α and such plots. The Urbach energy values for all the studied samples are calculated and tabulated in Table 2. The Urbach energy values for the studied glasses are found in the range from 0.2 to 0.38 eV. Mott and Davis [34] reported that, for the semiconductor amorphous materials, U values should be lying in the range from 0.045 to 0.67 eV. The refractive index, n, calculated from the value of E_{opt} using the formula proposed by Dimitro and Sakka [35] is as follows:

$$\left(n^2-1\right)/\left(n^2+1\right) = 1 - \left(E_{opt}/20\right)^{1/2}$$

The values of the refractive index for all the studied glass samples are calculated and tabulated in Table 2. It clears that by increasing Bi_2O_3 content, the refractive index increases slightly. This attributed to large atomic weight, coordination number of Bi_2O_3 and high polarizability of the Bi_3+ions [36] in the glass system as well as the more ionic refraction of Bi ions present in the glass.

To understand better the effect of composition on the refractive index, the empirical relation is derived by Lorentz [37] and Lorenz [38] used to estimate the molar refraction (R_m).

$$R_m = \frac{(n^2-1)}{(n^2+2)}\left(\frac{W}{\rho}\right)$$

where W is the average molecular weight and ρ is the density of the glass.

The theoretical optical energy gap is calculated using the relation [25]

$$E_{opt} = 20\left(1 - \left(R_m/V_m\right)\right)^2$$

Table 2 clears that the E_{opt} theoretical values larger than the experimental values, this is due to the amorphous nature of glass samples studied.

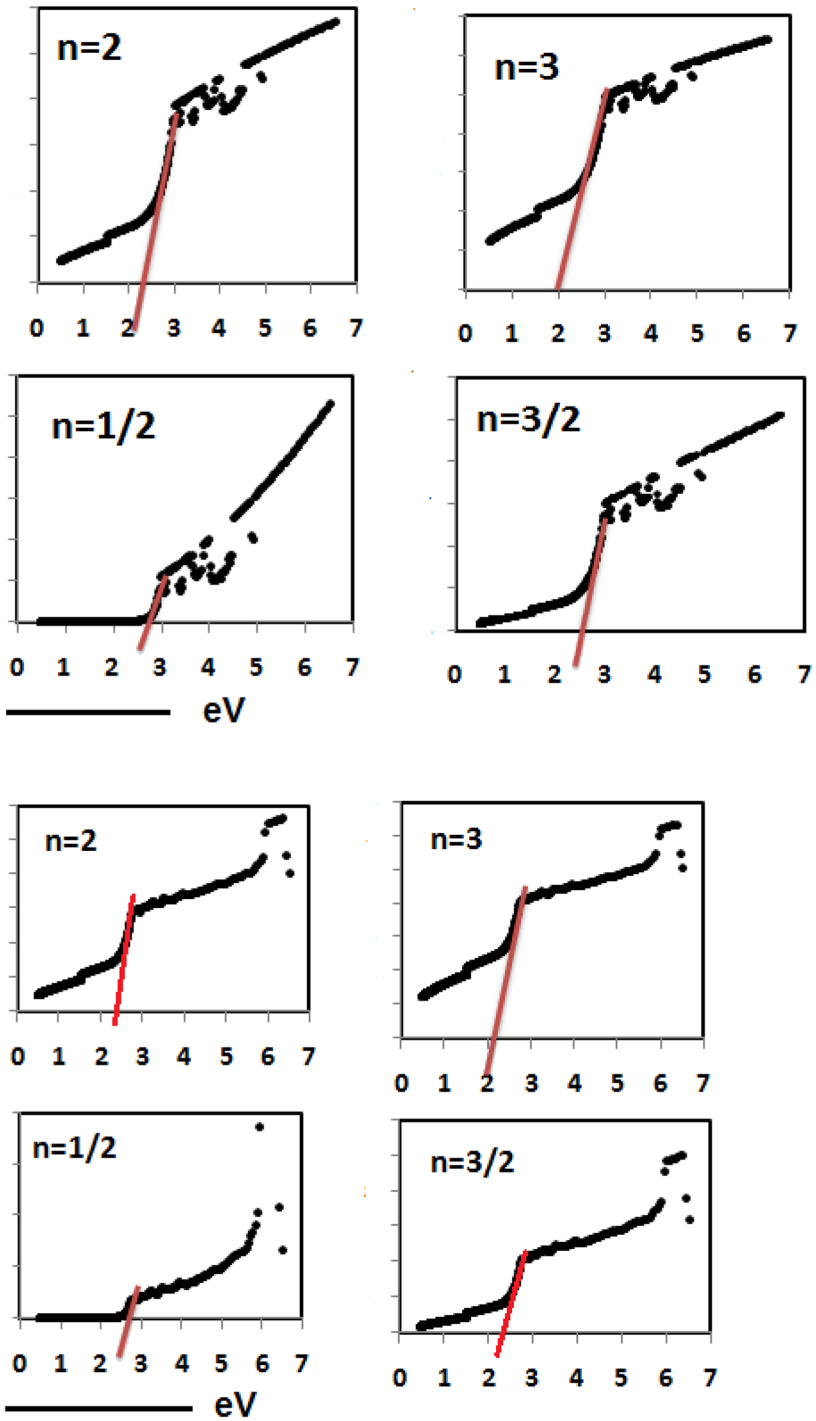

Fig. 8 dependence of $(\alpha h\nu)1/n$ on the photon energy $(h\nu)$ of the glass samples containing 45 and 85 mol% Bi_2O_3

Table 2 Optical energy gap E_{opt}, Urbach energy U(eV), and refractive index n for all the studied glass samples

Sample Bi_2O_3, mol%	E_{opt} (eV) exp.				E_g. n	U (eV)	E_{opt} (eV) Th.		Transition weather n, Mod.
	1/2	3/2	2	3			Th.	Th., Mod.	
45	2.8	2.4	2.3	2.0	2.98	0.30	4.71	2.98	3/2
55	2.8	2.4	2.1	1.7	3.05	0.38	4.80	3.04	3/2
65	2.8	2.5	2.4	2.0	2.95	0.27	4.67	2.96	3/2
75	2.8	2.4	2.3	1.9	2.9	0.25	4.60	2.92	3/2
85	2.7	2.4	2.25	1.6	2.75	0.20	4.40	2.79	3/2

The metallization criterion (metallic and nonmetallic of glass nature) depend on the refractive index and band gap energy is calculated and explained [24] on predating the nature of solids. The nature of solids metallic or nonmetallic based on the condition of the ratio (molar refraction /molar volume) < 1 (insulator) and > 1 (metal), by using the following equation [25],

$$M = 1 - (\text{molar refraction}/\text{molar volume})$$
$$M = R_m/M_v$$
$$M = 1 - (n^2 - 1)/(n^2 + 2)$$
$$M = (E_{opt}/20)^{(0.5)}$$

The metallization parameter M is calculated and listed in Table 3. It is clear that the metallization parameter values of the present glasses are found lesser than one and thus all the studied samples exhibit insulating behavior [25].

Molar refraction (R_m) linked with the glass structure and proportional to the electronic polarizability [39] of the glass α_m, as:

$$\alpha_m = \frac{3}{4\pi N} R_m$$

where N is the Avogadro number ($N = 6.023 \times 10^{23}$) that relates to the number of polarizable ions per mole. The ease of deformation of electronic clouds in the structure upon application of an electromagnetic field gives a measure of the ion electronic polarizability. Multiple properties of a material are defined by the electronic polarizability, such as refraction, conductivity, optical basicity along with optical nonlinearity, electro-optical effect, and ferroelectricity.

In this system, the lone pair of electrons present in the outermost shell of Bi^{3+} induces polarization on the application of an electric field or interaction with light. This type of interaction can govern a nonlinear response in these types of glass systems. In conventional optics, a linear relationship observed between the induced polarization (P) and the applied electric field (E), as,

$$P = \varepsilon_o x^{(1)} E$$

where $x^{(1)}$ is the linear susceptibility and ε_o is the free-space permittivity. And in nonlinear optics describes as:

$$P = \varepsilon_o[x^{(1)}E + x^{(2)}E + x^{(3)}E + \cdots]$$

where $x^{(2)}$ and $x^{(3)}$ are known as the second- and third-order nonlinear optical susceptibilities, respectively. Since glass is an isotropic material, with inversion symmetry $x^{(2)}$ becomes zero. On the other hand, third-order nonlinear optical interactions (described by the $x^{(3)}$ susceptibility) are observed in both centrosymmetric and non-centrosymmetric mediums. Third-order susceptibility $x^{(3)}$ is estimated according to the equation derived by Vogel et al. [40] as:

$$x^{(3)} = \frac{n}{12\pi}. n_2 = \frac{17}{3\pi}. \frac{\left[(n-1)\left(n^2+2\right)^2\right]}{v\left[1.52 + \frac{(n^2+2)(n+1)v}{6n}\right]^{0.5}}$$

where n is glass refractive index at 587.6 nm and n2 is a nonlinear refractive index that are approximated from the empirical relation derived by Vogel et al. According to the semi-empirical equation derived by Boling's [41], both the nonlinear refractive index (n2) and the linear refractive index (n) gives a measure of the $x^{(3)}$ material value. The third-order nonlinear susceptibility $x^{(3)}$ estimated by this equation [42]

$$x^{(3)} = \left[x^{(1)}\right]^4 \times 10^{-10}$$

where $\chi^{(1)}$ is the linear optical susceptibility calculated in accordance with

$$x^{(1)} = (n^2 - 1)/4\pi$$

The values of $x^{(3)}$ for the studied glass samples are calculated and given in Table 3. From Table 3 it is clear that the high values of third-order nonlinear optical susceptibility are located in the range [(0.38–0.53) × 10^{-12} esu], this means that all the studied samples are good applicants for nonlinear optical applications [42].

The third-order nonlinear optical susceptibility $x^{(3)}$ of materials is dependent on both the nonlinear refractive index (n2) and linear refractive index (n). The theoretical optical basicity (A_{th}), addresses the ability of oxide glass in contributing the negative charges in the glass matrix. In other words, it defines the electron-donating power of the oxygen in the oxide glass. The theoretical optical basicity (A)

Table 3 Molar polarizability, molar refraction, χ^3 third-order non-linear susceptibility, Ath optical basicity, α_{02-} ion polarizability, $M_{optical}$, M_{from} n metallization from optical energy gap and from refractive index, linear and nonlinear refractive index for all the studied samples

Sample Bi_2O_3, Mol%	Molar polariz-ability	$\chi^3 \times, 10^{-13}$ esu	A_{th}	α_{02-}	M_{Eop}	M_n	$R_{m,}$ (cm^3/mol)	n	n2, $\times 10^{-12}$
45	9.19	4.12	0.813	1.949	0.386	0.469	23.17	2.04	7.58
55	9.83	3.82	0.886	2.130	0.391	0.485	24.77	2.03	7.08
65	10.09	4.25	0.959	2.348	0.384	0.490	25.43	2.05	7.81
75	10.47	4.50	1.032	2.616	0.381	0.483	26.38	2.06	8.21
85	11.11	5.33	1.104	2.952	0.371	0.480	27.99	2.10	9.58

is calculated according to the approach proposed by Duffy and Ingram [43].

$$A_{\text{th}} = x(\text{SiO}_2)A(\text{SiO}_2) + x(\text{B}_2\text{O}_3)A(\text{B}_2\text{O}_3) + x(\text{Bi}_2\text{O}_3)A(\text{Bi}_2\text{O}_3) + x(\text{TeO}_2)A(\text{TeO}_2)$$

where $X(SiO_2)$, $X(B_2O_3)$, $X(Bi_2O_3)$ and $X(TeO_2)$ are the equivalent fraction of the different oxides, i.e., the proportion of the oxide atom that contributes to the glass system; $A(SiO_2)$, $A(B_2O_3)$, $A(Bi_2O_3)$ and $A(TeO_2)$ are the optical basicity values of the constituent oxides. Here, the values of $A(SiO_2)$ is 0.50, $A(B_2O_3)$ is 0.425, $A(Bi_2O_3)$ is 1.19 and $A(TeO_2)$ is 0.93 taken from the literature [25].

Table 3 collected the theoretical optical basicity values of glass samples. It clears that with the increasing Bi_2O_3 content, the theoretical optical basicity values increase. This increase due to Bi^{+3} ions possesses a lone pair in the valence shell, and therefore, the non-bridging oxygen increase with the increase the Bi^{+3} ion concentration. The increased optical basicity of the glasses with large Bi_2O_3 content indicates that the acid–base properties of Bi_2O_3 have a significant effect. The high optical basicity means high electron donor ability of the oxide ions to the cations [22].

The relationship between electronic polarizability of oxide ions a_{02-} and optical basicity of oxide *Ath* given by this equation [25]

$$a_{02-} = \frac{1.67}{1.67 - A_{\text{th}}}$$

The oxide ion electronic polarizability is determined and listed in Table 3. Table 3 clears that the oxide ion electronic polarizability increases by increasing Bi_2O_3.This means that the increasing Bi_2O_3 content caused the non-bridging oxygen increases, which makes the glasses become more polarized.

4 Conclusions

The bismuth oxide substituted by silicon and boron oxides decreases the glass-transition temperature values. The Hruby's parameter $K_{gL,}$ for all the studied samples decreases by increasing Bi_2O_3 content and is greater than 0.1. The optical band gap decreases with the increasing of Bi_2O_3 content.. The optical band gap E_{opt} (Tauc's method) far from the $E_{\text{opt}}(\lambda_g)$, (Photon energy's method) indicates that the Tauc's method is not correct for all compounds. The optical band gap $E_{\text{opt}}(M)$[my method] from the absorption coefficient α or n or k is closed to the optical band gap (photon energy's method) (λ_g) and is more accurate. Studied samples have higher values of third-order nonlinear optical susceptibility (3.82–5.33) × 10^{-13} esu which indicates that the all studied samples are good candidates for nonlinear optical applications. And the nonlinear refractive index change from (7.08 to 9.58) × 10^{-12} for studied samples.

The increasing Bi_2O_3 content, the present glasses becomes more basic. The metallization parameter values of the present glasses are found lesser than one and thus all the studied samples exhibit insulating behavior.

References

1. I. Opera, H. Hesse, K. Betzler, Opt. Mater. **26**, 235 (2004)
2. I. Pal, A. Agarwal, S. Sanghi, M.P. Aggarwal, Alloys Compds, **509**, 7625 (2011)
3. P. Becker, Cryst. Res. Technol. **38**, 82 (2003)
4. M. Shappan, Int. J. Thin Film Sci. Tech. **6**, 45 (2017)
5. M.G. Moustafa, Ceram. Int. **42**, 17723 (2016)
6. K. Maur, K.J. Singh, V. Ananol, Radiat. Phys. Chem. **120**, 63 (2016)
7. S.b.. Mallur, T. Czarnecki, A. Adhikari, P.K. Badu, Mater. Res. Bull. **68**, 27 (2015)
8. T.R. Taasheva, V.V. Dimitrov, Bul. Chem. Commun. **499**, 43 (2017)
9. T. Lin, Q. Yang, J. Si, T. Chen, F. Chen, X. Wang, X. Hou, K. Hiraa, Opt. Comm. **275**, 230 (2007)
10. T.A. Oliveira, D. Manzani, E.L. Falcao-Filho, Y. Messaddeq, G. Boudebs, K. Fedus, C.B. de Araújo, Appl. Phys. B **116**, 1–5 (2014)
11. Y. Li, Q. Zhang, J. Song, X. Gao, W. Tang, A. Lu, Non Cryst. Solids **483**, 43–49 (2018)
12. Z. Xu, Q. Guo, C. Liu, Z. Ma, X. Liu, J. Qiu, Appl. Phys. B **122**, 259 (2016)
13. G. Jagannath, B. Eraiah, K. Naga Krishnakanth, S. Venugopal Rao, J. Non Cryst. Solids **482**, 160–169 (2018)
14. J. Zhang, Q. Nie, S. Dai, T. Xu, F. Chen, X. Shen, X. Wang, J. Wuhan, Univ. Technol. Mater. Sci. Ed. **26**, 61–64 (2011)
15. S. Rani, N. Sanghi, A. Ahlawat, A. Agarwal, J. Alloy. Compd. **597**, 110–118 (2014)
16. Q. Che, H. Yang, L. Lu, Y. Wang, J. Alloys Compd. **549**, 221–225 (2013)
17. J.H. Yi, H.Y. Koo, J.H. Kim, Y.N. Ko, Y.J. Hong, Y.C. Kang, H.M. Lee, J. Alloys Compd. **509**, 6325–6331 (2011)
18. X. Zhu, C. Mai, M. Li, J. Non-Cryst. Solids **388**, 55–61 (2014)
19. V.C. Veeranna Gowda, Phys. B **426**, 58 (2013)
20. A. Bhogi, R.V. Kumar, P. Kistaiah, J. Non-Cryst. Solids **426**, 47 (2015)
21. I. Kashif, A. Ratep, S.K. El-Mahy, Mater. Res. Bull. **89**, 273–279 (2017)
21. A. Hruby, Czech J. Phys. B **22**, 1187 (1972)
22. S.P. Singh, B. Karmakar, Mater. Sci. Technol. Chap. 9, p 229 (2012)
23. B.V.R. Chowdari, P.P. Kumari, J. Phys. Chem. Solids **58**, 515 (1997)
24. V. Dimitrov, T. Komatsu, J. Chem. Tech. Metall. **48**, 549 (2013)
25. V. Dimitrov, T. Komatsu, J. Univ. Chem. Technol. Metall. **43**, 219 (2010)
27. E.A. Davies, N.F. Mott, Philos. Mag. **22**, 903 (1970)
28. N.F. Mott, E.A. Davis, Electronic processes in nor crystalline materials, 2nd edn. (Clarendon press, Oxford, 1979)

29. P. Pascuta, S. Rada, G. Borodi, M. Bosca, L. Pop, E. Culea, J. Mol. Struct. 924–926:214–220 (2009)
30. N. Srinivasa Rao, L. Srinivasa Rao, Y. Gandhi, V. Ravikumar, N. Veeraiah, Phys. B **405**, 4092–4100 (2010)
31. I. Kashif, A. Ratp, Opt. Quant. Electron **49**, 231 (2017)
32. M.N. Azlan, M.K. Hlimah, S.Z. Shafinas, W.M. Daud, Chalcogenide Lett. **11**, 319 (2014)
33. F. Urbach, Phys. Rev. **92**, 1324 (1953)
34. J.R. Macdonald, *Impedance Spectroscopy Emphasizing Solid Material and Analysis* (Wiley, New York, 1987)
35. V. Dimitrov, S. Sakka, J. App. Phys. **79**, 1741 (1996)
36. V. Dimitrov, J. Appl. Phys. **79**, 1736 (1996)
37. H.A. Lorentz, Ann. Phys. **9**, 641–665 (1880)
38. R. Lorentz, Ann. Phys. **11**, 70–103 (1880)
39. M.V. Shankar, K.B.R. Varma, Mater. Res. Bull. **33**, 1769–1782 (1998)
40. E.M. Vogel, M.J. Weber, D.M. Krol, Phys Chem Glass **32**, 231–254 (1991)
41. N.L. Boling, A.J. Glass, A. Owyoung, IEEE J. Quantum Electron. **14**, 601–608 (1978)
42. T. Tashera, V. Dimitrov, J. Chem. Technol. Metall. **50**, 441 (2015)
43. J.A. Duffy, M.D. Ingram, *Optical Properties of Glass*, vol. 5. (The American Ceramic Society, 1991), pp. 159–184